

Design and correlation analysis of quasi-zero stiffness passive vibration isolation air spring

Jiayue Wu

Beihang University, Beijing, China

20376028@buaa.edu.cn

Abstract: Vibration isolation systems are widely used in high-end automobile manufacturing, precision instrument processing, building and bridge seismic resistance, ship machinery noise reduction and other engineering fields, with good development prospects. At present, the existing vibration isolation systems on the market are mainly divided into active and passive vibration isolation systems. Passive vibration isolation does not require external energy input. Its structure is simple and the control scheme is easy to implement. However, passive vibration isolation performs well in high frequency vibration but not in low frequency. As a new nonlinear low-frequency vibration isolation technology, the quasi-zero stiffness vibration isolation system has changed the traditional concept of linear system vibration isolation. In addition, compared with traditional spring, air spring as a new type of elastic vibration isolation mechanism has many excellent performances, such as high fatigue resistance and high stiffness. Therefore, this paper uses air spring to design a passive vibration isolation quasi-zero stiffness air spring structure with good vibration isolation effect, simple structure and low cost in both low-frequency and high-frequency vibration.

Keywords: quasi-zero stiffness, air spring, shock isolation.

1. Introduction

In the high-end automobile manufacturing industry, the vibration isolation system has always been a hot research topic [1]. On the one hand, a good vibration isolation system can reduce the vibration noise caused by engine torque excitation and tire noise caused by road excitation. On the other hand, it can greatly improve the driver's comfort, so that the driver and passengers can be stable even under uneven road conditions [2]. In addition, the vibration isolation system is also widely used in precision instrument processing, house bridge earthquake resistance, vehicle engine, marine machinery noise reduction and other engineering fields, with good development prospects [3].

Based on the broad application prospects of the vibration isolation system, this paper plans to design and mechanically process a set of quasi-zero stiffness air spring system to achieve basic vibration isolation. As an emerging nonlinear low-frequency vibration isolation technology, the quasi-zero stiffness isolation system has changed the traditional concept of vibration isolation of linear systems [4]. The quasi-zero stiffness isolation system is composed of a positive and negative stiffness structure in parallel. The positive stiffness structure can provide carrying capacity. The negative stiffness structure is mainly used to reduce the total stiffness of the system, so that the total stiffness value of the whole vibration isolation system is close to zero, that is, quasi-zero stiffness [5,6]. The basis of its realization is that the force on the vertical plane of the system causes the spring to deform in the horizontal plane,

and there is no deformation or displacement in the vertical plane.

At present, the existing vibration isolation systems on the market are mainly divided into active and passive vibration isolation [7]. Passive vibration isolation does not require external energy input, the structure is simple and the control scheme is easy to implement. However, the existing problem is that the passive vibration isolation performs well at high frequencies, but not well at low frequencies [8]. Therefore, the goal of our design is to achieve a passive quasi-zero stiffness mechanical structure, so that it has excellent performance in both low-frequency and high-frequency vibration reduction.

In addition, the air-spring vibration isolator is a new type of elastic vibration isolation mechanism that can achieve elastic effect by filling compressed air into the closed airbag[9]. Compared with traditional springs, air springs have many excellent properties, such as high fatigue resistance and high stiffness [10]. Therefore, this paper uses air spring to design a quasi-zero stiffness air spring with good vibration isolation effect, simple structure and low cost in both low-frequency and high-frequency vibration.

2. Introduction of a new type of quasi-zero stiffness passive vibration isolation air spring mechanism

At present, most of the vibration damping springs have good damping effect at high frequencies, but they perform poorly at low frequencies. In this paper, a new structure is adopted, that is, the shape of the supports on both sides is designed as M-shaped (composed of two V-shaped supports), and three air springs are connected in the middle. The upper and lower U-shaped are respectively the support and the vibration disturbed parts. The overall structure is shown in Figure 1.

Among them, the connecting pieces in the middle, namely the four V-shaped supports, is connected by three supporting pieces (i.e., two pieces clamp one piece, as shown in Figure 2) to reduce the weight of the whole mechanism, and the angle between the three supporting pieces that constitute the V-shaped rod is kept constant through the connection of the angle adjusting rod during the movement of the mechanism.

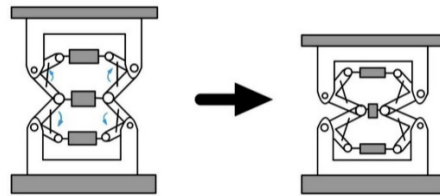


Figure 1. Model of new vibration damping mechanism.

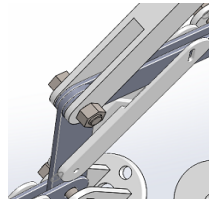


Figure 2. Connection diagram at V-shaped rod.

However, the two V-shaped rods that make up the left and right M-shaped mechanisms can rotate relatively. Thus, when the whole platform is disturbed by vibration, four V-shaped rods will rotate symmetrically from left to right, up and down, so as to compress the air spring, take the resistance of the air spring as the power to reduce vibration, and achieve the effect of quasi-zero stiffness spring.

2.1. Institutional innovation

2.1.1. The angle between V-shaped plates can be adjusted. The included angle between the connecting L-shaped rods on both sides needs to ensure that the rigidity of the structure is close to 0. However, the included angle that meets the conditions is not exactly 90 degrees calculated by Matlab, and the included angle that is not 90 degree is difficult to mill. Therefore, this paper designs an angle positioning splint.

A rod is added to the vertical, and the included angle is positioned with the screw nut to realize the adjustable angle and accurate positioning, as shown in Fig. 3 and Fig. 4.

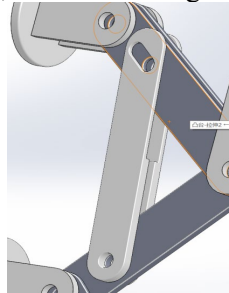


Figure 3. Schematic diagram of angle adjustment plate.

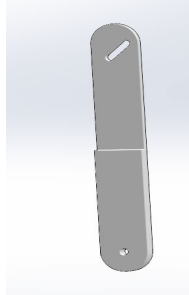


Figure 4. Part drawing of angle adjusting plate.

2.1.2. Convert transverse stiffness into longitudinal quasi-zero stiffness. In the structure designed in this paper, the air spring is placed horizontally so its stiffness is horizontal. It can provide buffer for lateral external forces. However, the structure uses a hinge connecting rod to connect the air spring with the external structure, and uses a rotatable L-shaped rod to convert the horizontal tension and compression of the spring into vertical up and down movement, which can reduce the vertical vibration common in life, as shown in Figure 5.

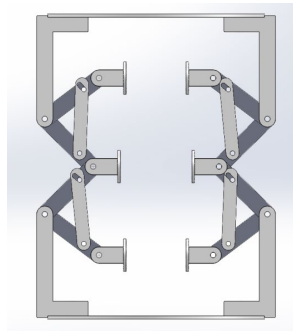


Figure 5. SolidWorks assembly drawing of damping spring.

2.1.3. Use air spring to make the mechanism performance better. The traditional damping system is designed with ordinary coil spring, but the air spring often used in cars has better damping effect than coil spring. Unlike ordinary shock absorbers, the air spring mainly relies on the top rubber to compress the air to achieve the shock absorption effect. Many precision mechanical equipment must use air springs to achieve the real shock absorption effect of the equipment. Through the internal height control of the air spring, the height of the air spring can be kept consistent under any load, so the air spring can adapt to a variety of working environments and temperatures. The air spring also has the characteristics of good sound absorption and insulation effect, and will not generate noise during operation.

Air spring has excellent nonlinear hard characteristics, so it can effectively limit the amplitude, avoid resonance and prevent impact. The natural frequency of the air spring vibration isolation system can be designed to be very low, even below 1 Hz, while the natural frequency of the rubber vibration isolator

is generally 5~7 Hz. Therefore, the vibration isolation efficiency of air spring is much higher than that of other vibration isolation elements, and it can isolate low-frequency vibration.

Therefore, in this paper, air spring is used to replace the traditional spring, and the number of springs is designed to be three, so that three times of compression elongation can be obtained. According to Hooke's law, three times of displacement corresponds to three times of external load. Through this method, the mechanism with three times of damping effect can be made. The physical picture of air spring is shown in Figure 6 and Figure 7.



Figure 6. Right aerial view of air spring. **Figure 7.** Left aerial view of air spring.

2.2. Static theoretical analysis of mechanism

2.2.1. Calculation and analysis of damping mechanism stiffness. The main structure of the spring and the corresponding rod number are shown in Figure 8:

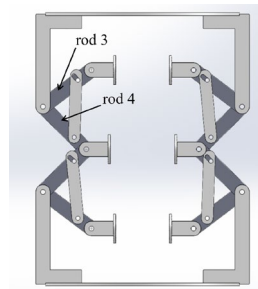


Figure 8. Main structure of spring and number of corresponding rod
The parameters of air spring are shown in Table 1:

Table 1. Parameters of air spring

Parameter	Data
100mm	100mm
Initial height H	130mm
Air pressure P	One standard atmospheric pressure~eight standard atmospheric pressure
Quality M	1.33KG
Maximum compression X	30mm

As a passive nonlinear vibration isolator capable of isolating low-frequency vibration, quasi-zero stiffness vibration isolator has very important research value. In order to achieve the quasi-zero stiffness of the structure, the design method is needed to obtain the angle between the three and four bars so that the whole system can achieve the quasi-zero stiffness in any state.

Let y be the displacement of the loading plate from the initial position to any position, assuming θ is the angle between the initial 3 poles and the vertical direction, θ_1 is the angle formed after pressurization, α is the angle between 3 and 4 bars, initially $2\theta + \alpha = 180^\circ$. The length of 3 rods and 4 rods is l . α is the angle need to be calculated, which do not change during the experiment. The structure is shown in

Figures 9 and 10.

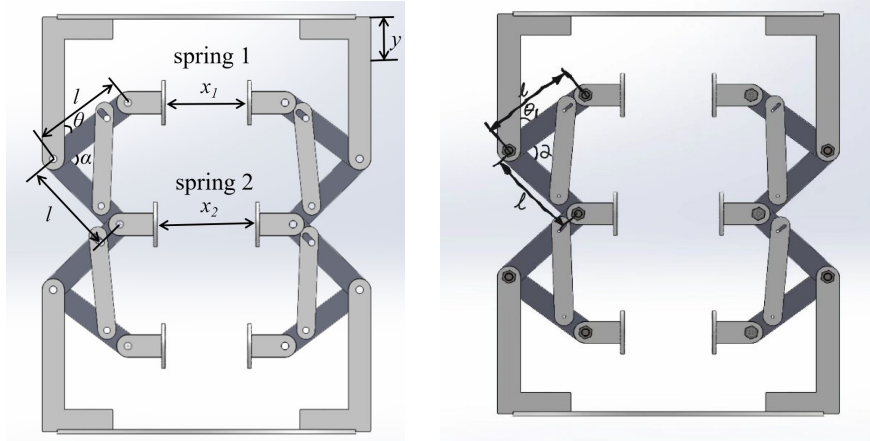


Figure 9. Before spring deformation.

Figure 10. After spring deformation.

Order Δx is the changed length of the air spring, as shown in Figure 11. The deformation of air spring 1 and 2 can be calculated respectively according to the structural changes before and after deformation:

$$\Delta x_1 = 2l(\sin\theta - \sin\theta_1) \quad (1)$$

$$\Delta x_2 = 2l[\sin(\alpha + \theta_1) - \sin(\alpha + \theta)] \quad (2)$$

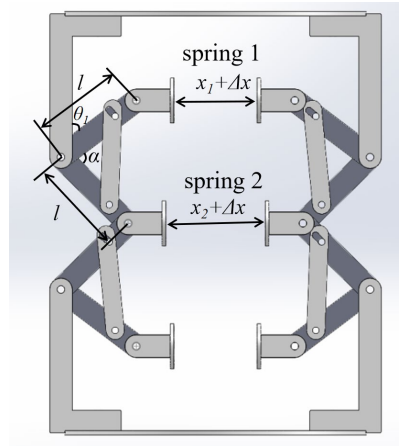


Figure 11. Variation of spring after deformation.

According to the overall structure change, the vertical direction change is:

$$\frac{y}{2} = l[\cos(\alpha + \theta_1) - \cos(\alpha + \theta)] \quad (3)$$

Let the force generated by the air spring be F_S . Assuming that the three air springs can be directly linear simulated, and the elastic modulus is k , then F_{S1} can be obtained from Formula 1 and 3, and F_{S2} can be obtained from Formula 2 and 3, that is, the force formed after the air spring is pressurized is respectively:

$$F_{S1} = k\Delta x_1 = k \frac{y(\sin\theta - \sin\theta_1)}{\cos(\alpha + \theta_1) - \cos(\alpha + \theta)} \quad (4)$$

$$F_{S2} = k\Delta x_2 = k \frac{y[\sin(\alpha + \theta_1) - \sin(\alpha + \theta)]}{\cos(\alpha + \theta_1) - \cos(\alpha + \theta)} \quad (5)$$

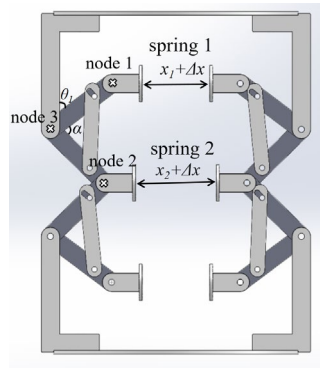


Figure 12. Each node of the spring.

It is assumed that when the pressure is balanced, the force in the vertical direction is F_N , the force generated by three rods is F_3 , and the force generated by four rods is F_4 .

As shown in Figure 12, formula 6 is obtained for force analysis at node 1, formula 7 is obtained for force analysis at node 2, and formula 8 is obtained for force analysis at node 3:

$$F_3 \sin \theta_1 = F_{S1} \quad (6)$$

$$2F_4 \sin(\alpha + \theta_1) = F_{S2} \quad (7)$$

$$\frac{F_N}{2} = F_3 \cos \theta_1 + F_4 \cos(\alpha + \theta_1) \quad (8)$$

The formula for calculating the spring stiffness is:

$$K = \frac{dF_N}{dy} \quad (9)$$

2.2.2. V-bar included angle simulation and calculation. By calculating the stiffness K and generating a three-dimensional surface graph through traversing, a curved surface is produced that illustrates the changes in stiffness K relative to θ , as depicted in Figure 13. To pinpoint the position where stiffness is closest to zero, as shown in Figure 14, identify the point in three-dimensional space where stiffness approaches zero (as demonstrated in Figures 15 and 16). Since springs are generally stable, with amplitudes not being excessively large, the solution must be found near the diagonal of the coordinate system. Consequently, the rightmost curved surface in the figure is selected. Upon further magnification of the surface, it can be observed that the value remains relatively stable around 0.8301 radians.

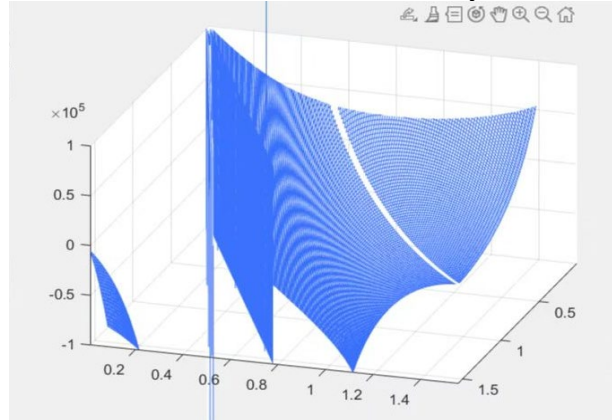


Figure 13. Surface of stiffness K varying with θ .

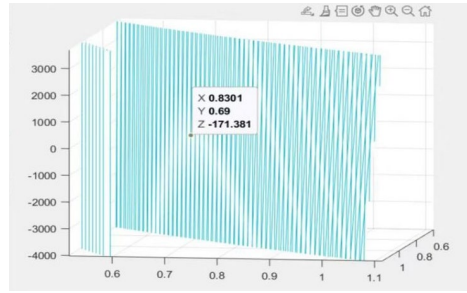


Figure 14. Stiffness closest to zero.

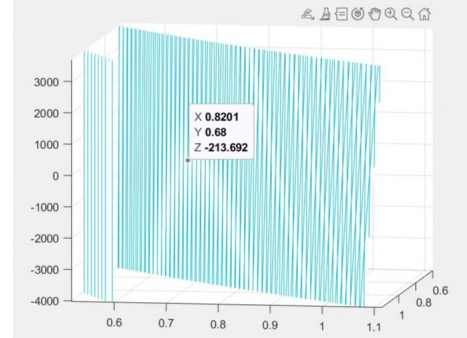


Figure 15. The best position is 0.01 radian to the left.

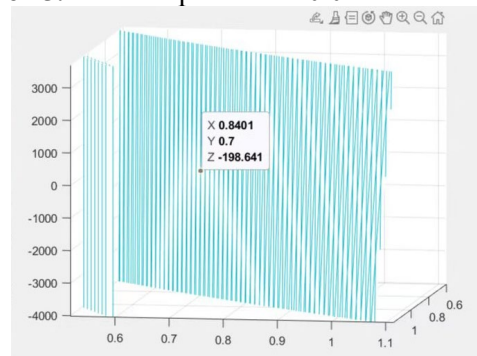


Figure 16. The best position is 0.01 radian to the right.

The theoretical value of the parameter θ can be determined as 47.55° .

2.3. Dynamic theoretical analysis of mechanism

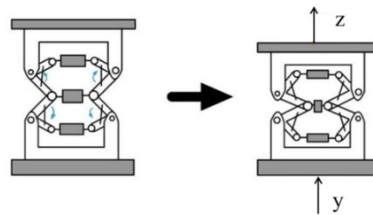


Figure 17. Structural diagram of dynamic theoretical analysis.

Define functions:

$$F(\theta) = \cos(\theta + \alpha) \quad (10)$$

$$g(\theta) = \sin(\theta) \quad (11)$$

$$A(\theta) = \sin(\theta + \alpha) \quad (12)$$

As shown in Figure 17, Laplace transformation is adopted by combining the formula in 1.2.1 with Newton's second law,

For springs:

$$\frac{y-z}{2} = [sF(s) - \cos \alpha] \cdot l \quad (13)$$

$$F_{s1} = k \cdot \frac{ys \cdot g(s)}{sF(s) - \cos \alpha} \quad (14)$$

$$F_{s2} = k \cdot \frac{ys \cdot A(s)}{sF(s) - \cos \alpha} \quad (15)$$

$$msZ(s) = F_{s1} \cos \theta + F_{s2} \cos(\theta + \alpha) = F_{s1} \quad (16)$$

The force analysis of the upper platform includes:

$$m\ddot{z} = \frac{ky}{\cos(\theta+\alpha+d\theta)-\cos(\theta+\alpha)} \{[\sin \theta - \sin(\theta + d\theta)] \cos \theta + [\sin(\alpha + \theta + d\theta) - \sin(\alpha + \theta)] \cdot \cos(\theta + \alpha)\} \quad (17)$$

$$\frac{y-z}{2} = l \cdot [\cos(\theta + \alpha + d\theta) - \cos(\theta + \alpha)] \quad (18)$$

$$msZ(s) = \frac{2kYL}{Y-Z(s)} \quad (19)$$

Available:

$$Z = \frac{msY + \sqrt{m^2s^2Y^2 - 8mskYL}}{2ms} \quad (20)$$

$$msZY - msZ^2 = 2kYL \quad (21)$$

$$msZ^2 - msYZ + 2kYL = 0 \quad (22)$$

The dynamic characteristic formula is obtained as above.

3. Entity model of mechanism

In the actual research process, two methods are used to construct the spring system. Although the strength and durability of the parts processed in the workshop are better, the processing is slightly cumbersome. If there is no sufficient analysis and verification, the hasty labor union will cause a great waste of financial, material and human resources. Therefore, a mini spring system is first produced by 3D printing. After the structure is determined to effectively reduce the overall stiffness of the spring through more than half quantitative experiments, aluminum alloy blanking is used in the workshop with the help of a lathe Milling machines and drilling machines are used to process solid mechanical parts.

3.1. Additive manufacturing solid model

The basic structure design of the mechanism for 3D printing is the same as that of the air spring, but the larger air spring is replaced by the smaller nitrogen spring. The overall size is scaled down and the structure is adjusted according to the actual situation for 3D printing. The overall modeling structure is shown in Figure 18, and the basic size is shown in Figure 19:

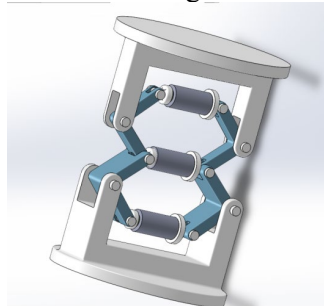


Figure 18. Structure diagram of nitrogen spring.

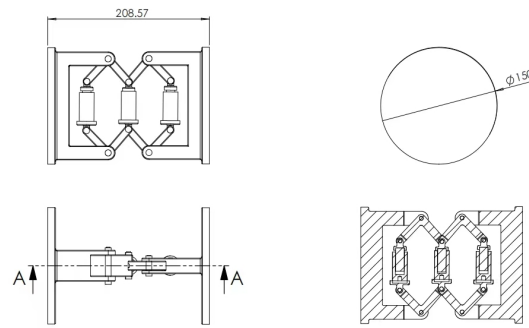


Figure 19. Basic size diagram of nitrogen spring structure.

Because the nitrogen spring itself is too rigid to be compressed during actual assembly, which makes the mechanism unable to carry out the ideal movement and has no more benefit for verifying the correctness of the air spring structure, this paper replaces the nitrogen spring with an ordinary spring with a smaller stiffness but still has a larger stiffness than the nitrogen spring. As shown in Figure 20, the hooks at both ends are consistent with the structure designed in this paper.



Figure 20. Structure diagram of common spring.

After semi-quantitative testing, the stiffness of the spring mechanism is significantly reduced as shown in Figure 21, which shows that the structural design of this paper has the potential to make the system reach "quasi zero".

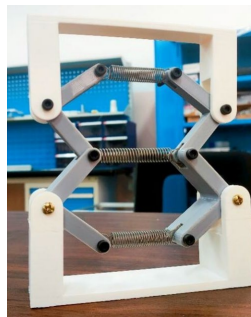


Figure 21. 3D printing damping spring picture.

3.2. Machined solid model

Except for standard parts, all parts of mechanical parts are processed in the workshop. There are 8 groups of 32 parts to be processed in this paper. The important processes are described below.

3.2.1. Upper and lower bottom plates. First cut off the four corners of the square aluminum plate, and use the disk clamp to make a disc with a diameter of 400mm for the outer circle of the base plate. After the outer circle of the base plate is processed, clamp it on the vertical milling machine, and use the standard needle to align the drawn groove line. After the bottom plate outer circle is processed, clamp it on the vertical milling machine, and align the drawn groove line with the standard needle.

3.2.2. L-shaped plate. During initial blanking, 25mm thick aluminum plate is used for processing on the milling machine, and each piece is quickly milled with a face milling cutter to obtain a high-quality surface. The arc surface is completed by wire cutting, and finally the hole is punched on the drilling machine.

3.2.3. *Spring connector*. The difference between the left and right spring connectors is that the right connector needs two more fixing holes at last. Bore the hole while turning the outer circle, and then cut the allowance on the milling machine. During processing, the number of turns of the handwheel shall be strictly controlled, and the allowance for finishing milling and back chipping shall be reserved, and finally back chipping and arc milling shall be conducted.

3.2.4. *Angle fixing rod*. The angle fixing rod is mainly drilled by the drilling machine, and the arc, platform and fixing groove are cut by the wire cutting machine.

3.2.5. *Connecting rod*. There are two kinds of connecting rods, 3mm and 5mm thick, with the same processing process. The outer contour is milled to the drawing size by a milling machine at one time, and then the arc is cut by a wire cutting machine, and finally the hole is punched on the drilling machine.

4. Conclusion

At present, quasi-zero stiffness air spring is a research hotspot in the academic field, and there are few existing structures that can be referenced and developed rapidly. Through theoretical calculation and verification, Solidworks modeling, 3D printing model with nitrogen spring as the main body, and the final part processing and assembly test, this research has verified that the quasi-zero stiffness passive vibration isolation air spring rotates symmetrically from left to right, up and down in structure, so as to compress the air spring and take the resistance of the air spring as the power to reduce vibration, and achieve the effect of quasi-zero stiffness spring. It provides a new idea for the structure of quasi-zero stiffness air spring. However, this structure has large product volume and is too bulky; There are many parts, complex structure and time-consuming and laborious installation. And due to the limitation of research focus and space, it has not been tested and verified in real scenes, which is also the focus of this study in the next step, and further improve the structure on the original basis.

Reference

- [1] Causemann P. Modern vibration damping systems[J]. ATZ worldwide, 2003, 105(11): 10-13.
- [2] Du Y, Chen J, Zhao C, et al. Comfortable and energy-efficient speed control of autonomous vehicles on rough pavements using deep reinforcement learning[J]. Transportation Research Part C: Emerging Technologies, 2022, 134: 103489.
- [3] Chen Lijuan, Li Jinsong, Zhang Zhipeng Modeling and performance analysis of air spring seats * [J] Electromechanical Technology, 2013 (5): 24-26. DOI: 10.3969/j.issn.1672-4801.05.010
- [4] Liao Shijia, Wang Kao, Wu Yan, etc Comparative simulation study on performance of pneumatic vibration table [J] Mechanical Science and Technology, 2008,27 (6): 710-714 DOI:10.3321/j.issn:1003-8728.2008.06.003.
- [5] Ren Xudong Characteristic analysis and application research of air spring quasi-zero stiffness vibration isolator [D] PLA Academy of Military Medical Sciences, 2017
- [6] Zhang Xiao Research on four-corner interconnected air suspension and its interconnected state control method [D] Jiangsu: Jiangsu University, 2019
- [7] Li Zilong Research on structural dynamics analysis and design of high-performance active vibration isolation system [D] Hubei: Huazhong University of Science and Technology, 2015. DOI: 10.7666/d. D731201
- [8] Zhang Yilong Research on dynamic performance of air spring based on ANSYS [D] Shaanxi: Xi'an University of Architecture and Technology, 2015 DOI:10.7666/d.D01417047.
- [9] Yu Xuyang Research and experimental verification of stiffness adjustment method of split vibration isolator [D] Heilongjiang: Harbin University of Technology, 2021
- [10] Yin Zhihong. Theoretical and experimental study of double-chamber air suspension system [D] Hunan: Hunan University DOI:10.7666/d.d201112.